Interaction of wide-band-gap single crystals with 248-nm excimer laser irradiation. IX. Photoinduced atomic desorption from cleaved NaCl(100) surfaces

K. H. Nwe, S. C. Langford, and J. T. Dickinson[a)]
Physics Department, Washington State University, Pullman, Washington 99164-2814

(Received 28 April 2004; accepted 20 May 2004; published online 5 July 2005)

Neutral atomic sodium and chlorine emissions from cleaved, single-crystal NaCl(100) surfaces due to pulsed, 248-nm excimer laser irradiation have been characterized by time-resolved, quadrupole mass spectroscopy. At laser fluences below the threshold for optical breakdown, the resulting time-of-flight signals are consistent with particles emitted in thermal equilibrium with a laser-heated surface. Activation energy measurements made by varying the substrate temperature are consistent with *F-H* pair formation under UV excitation. By varying the laser fluence and estimating the effective surface temperature from the time-of-flight signals, additional activation energy measurements were made. The corresponding rate-limiting step is attributed to a thermally assisted, photoelectronic process involving atomic steps. Atomic force microscope images of surfaces irradiated at low fluences show monolayer islands that are created by the aggregation of material desorbed from steps. At somewhat higher fluences, monolayer pits due to *F*-center aggregation are also observed. © *2005 American Institute of Physics*. [DOI: 10.1063/1.1927701]

I. INTRODUCTION

Interactions between pulsed UV laser radiation and wide-band-gap single crystals have important applications in thin-film production, chemical analysis, and in the durability of optical components. Sodium chloride is a wide-band-gap ionic material, nominally transparent to UV photons with energies less than about 7 eV. Nevertheless, significant interactions with 5-eV photons are observed due to the presence of point defects.[1,2] Due to the importance of alkali halides as model ionic materials, the production of point defects during exposure to energetic electrons and photons has been extensively studied.[1,3–6] In vacuum, electronic excitations can lead to the emission of halogen atoms and molecules, either by diffusion of halogen-excess defects to the surface, or by the decay of excitations at the surface itself.[7–9] In the presence of surface defects, such as steps, electronic excitations can yield both alkali and halogen emissions, often yielding layer-by-layer material removal in the early stages of irradiation.[10–12] These processes are readily studied by using low fluxes of energetic electrons or photons, which yield relatively high densities of excitations and little surface heating.

The interaction of alkali halides with pulsed UV laser radiation is complicated by the transient nature of the excitation. To achieve detectable surface modification and emission, the instantaneous excitation densities and effective surface temperature must be much higher than when continuous sources of excitation are employed. Depending on the laser wavelength and the electronic structure of the alkali halide, excitations across the band gap are rare, with defects playing an important role in the absorption process. Therefore, it is often difficult to relate the processes observed during pulsed UV laser excitation with the fundamental mechanisms identified at low excitation densities.

In this work, we examine photoinduced neutral atom emission during exposure to pulsed 248-nm radiation (KrF excimer) at fluences well below those required for optical breakdown. We observe atomic sodium and chlorine in approximately stoichiometric amounts. We examine the intensities of these desorbed species as a function of background substrate temperature which permits an identification of a slow, thermally activated process that can greatly enhance these emissions. At constant background substrate temperature we are able to fit the desorbed atom time-of-flight curves to Maxwell–Boltzmann distributions which permit the determination of "desorption" temperatures. With the assumption that these values correspond to the transient surface temperatures under the laser beam, a second activation energy is determined which we interpret in terms of surface step modification processes. Finally, using atomic force microscopy of the laser-irradiated samples, we show and explain striking rearrangements of material by laser irradiation involving atomic step erosion, formation of monolayer islands, and eventually monolayer pits. This work shows that low laser fluence exposure of nominally transparent materials can lead to a rich set of surface modification phenomena.

II. EXPERIMENT

Cleavable, single-crystal NaCl from Optovac, Ltd. was cleaved into 1-mm-thick plates and mounted in vacuum on a stainless-steel support that could be resistively heated. The support temperature was measured by a Chromel-Alumel thermocouple spot welded to the back. Twenty minutes were allowed after each change in heating current to allow the sample to come into thermal equilibrium with the support.

[a)]Electronic mail: jtd@wsu.edu

Exposure to pulsed 248-nm radiation (KrF excimer, 5-eV photons, 30-ns pulse width) was carried out at pressures of about 10^{-7} Pa. Radiation from a Lambda Physik Lextra 200 excimer laser was focused to a 0.4×0.3 cm^2 spot on the sample. The fluence (energy per unit area per pulse) was determined by dividing the pulse energy, measured with a Gentec ED-500L joulemeter, by the spot area. A repetition rate of 1 Hz was used to minimize cumulative sample heating by the laser.

Desorbed neutral particles were detected with a UTI 100C quadrupole mass spectrometer (QMS) after electron-impact ionization (electron kinetic energy 70 eV) in an ionizer mounted at the entrance aperture of the mass filter. The long axis of the mass spectrometer was directed at the laser spot, perpendicular to the sample surface. The output of the Channeltron electron multiplier mounted at the exit aperture of the mass filter was amplified and pulse counted as with ions.

If a large number N of neutral particles in thermal equilibrium with a surface are emitted at time $t=0$, they will have an average particle density at point (x,y,x) and later time t given by

$$\rho(t)=\left(\frac{m}{2\pi kT}\right)^{3/2}\frac{Nx}{t^4}\exp\left[\frac{-m(x^2+y^2+z^2)}{2kTt^2}\right], \tag{1}$$

where m is the particle mass, T is the surface temperature, k is the Boltzmann constant, and $x>0$ is the distance from the plane of the surface. If the quadrupole ionizer is mounted along the surface normal opposite the point source $(y,z\approx0)$ at a distance d much greater than the dimensions of the quadrupole ionizer, the detected signal is given by

$$I(t)=\left(\frac{m}{2\pi kT}\right)^{3/2}\frac{\alpha NVd}{(t-t')^4}\exp\left[\frac{-md^2}{2kT(t-t')^2}\right], \tag{2}$$

where α is a constant that accounts for the ionization and transmission efficiencies, assumed to be constant over the volume V of the ionizer. The time t is the arrival time at the channel electron multiplier (CEM) detector relative to the laser pulse, t' is the flight time in the quadrupole mass filter; therefore $(t-t')$ is the flight time from the surface to the ionizer. The constant α can be determined by measuring the quadrupole output as a function of partial pressure of a gas whose mass is similar to that under study.

Irradiated surfaces of interest were imaged in air with a Digital Instruments Nanoscope III atomic force microscope (AFM) using commercial Si_3N_4 tips with cantilever force constants of 0.6 N/m.

III. RESULTS

A. Time-of-flight signals

At modest laser fluences, 248-nm irradiation of NaCl produces a variety of neutral products, including neutral Na, Cl°, and small amounts of neutral Cl_2 and NaCl. Typical time-of-flight (TOF) signals for neutral Na° and Cl° for the same laser fluence (120 mJ/cm^2) appear in Fig. 1. Consistent with their different masses, the Na° signal peaks well before the Cl° signal. This rules out, for instance, molecular NaCl as a major source for the two signals. Although the dissociation of molecular NaCl by electron impact in the quadrupole ionizer can produce signals at both 23 amu/e (Na) and 35 amu/e (Cl°), these signals (with appropriate corrections for differences in the time spent in the QMS mass filter as ions) would display the same TOF behavior. Furthermore, although a very small molecular NaCl signal was detected, its cracking fraction would not be detectable given our signal-to-noise ratio.

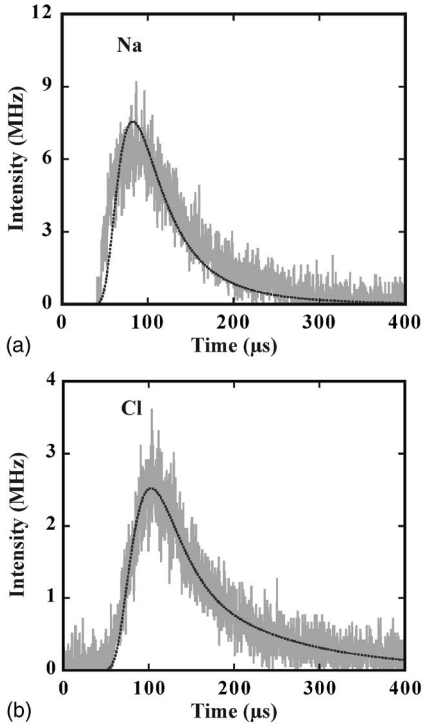

FIG. 1. Time-of-flight signals of neutral (a) Na° and (b) Cl° from single-crystal NaCl exposed to 120-mJ/cm^2 pulses of 248-nm radiation at a substrate temperature of 400 K.

Both atom emission signals are reasonably described by Maxwell–Boltzmann TOF distributions. Least-squares fits of Eq. (2) to the data of Fig. 1 are shown by the dark lines. Small but systematic departures from Maxwell–Boltzmann behavior are observed at both short and long times. Least-squares fits to the two signals (dark lines) yield quite similar temperatures, 2350 K for the Cl° signal and 2500 K for the Na° signal. The quality of the fits suggests that the great majority of both species are emitted in quasithermal equilibrium from a laser-heated surface at ~2400 K. Cooling following nanosecond laser-induced heating is relatively short (<1 μs). The high effective temperature of these emitted particles indicates that the great majority of emission occurs in this short sub-microsecond period of high surface temperature; we show below that the rates of neutral emission exhibit Arrhenius behavior corresponding to two independent thermally enhanced processes.

B. Emission intensities as a function of background substrate temperature

Raising the background substrate temperature typically raised the emission intensities and shifted the time-of-flight curves to slightly shorter times. Measurements of the inte-

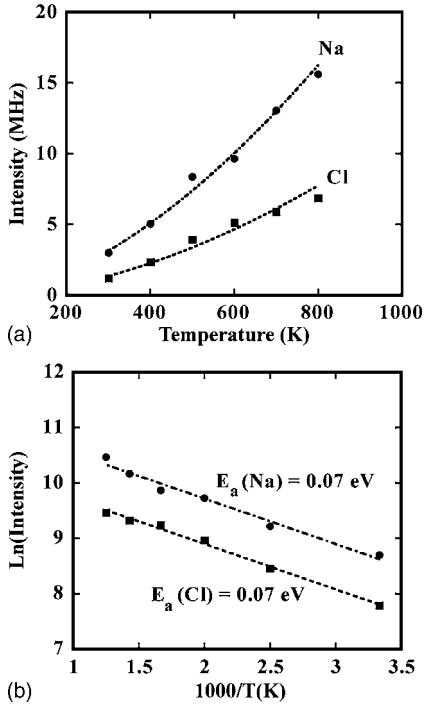

FIG. 2. Signal intensities vs background substrate temperature at a fluence of 120 mJ/cm^2 (a) linear plot and (b) Arrhenius plot.

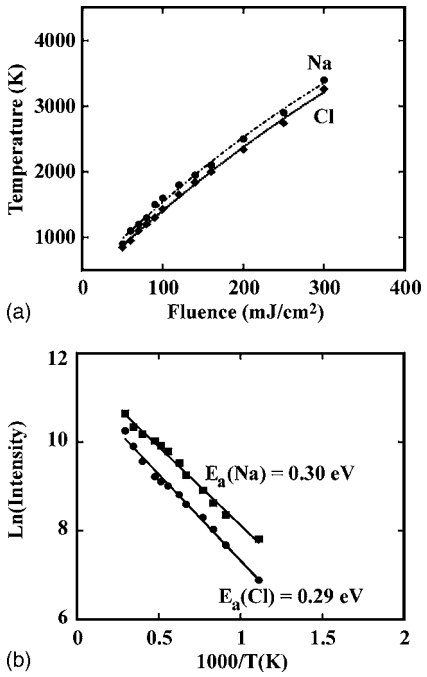

FIG. 3. (a) Effective surface temperatures derived from Maxwell–Boltzmann fits to Na° and Cl° time-of-flight data vs fluence and (b) Arrhenius plots of the emission intensities vs effective surface temperature. The background surface temperature was 300 K.

grated total counts detected at 23 and 35 amu/e for 50 laser pulses at a constant laser fluence as a function of substrate temperature are shown in Fig. 2(a) and plotted in Arrhenius form in Fig. 2(b). The intensity growth with substrate temperature yields from Fig. 2(b) an activation energy of 0.07 ± 0.01 eV for *both* Na° and Cl° emissions. This value is consistent with a known thermal activation energy for F-center formation in NaCl by ionizing radiation.[4] In Sec. III C, however, we show that particle emission itself takes place at much higher effective surface temperatures. Similar measurements made while introducing 10^{-5}-Pa water vapor (which can interact only with the surface) into the vacuum system show no change in apparent activation energy. Thus it is likely that the relevant thermally activated process responding to these changes in the background crystal temperature is due to processes confined to the sample interior. We argue that this process, which can continue long after the laser pulse, is responsible for generating *more* emission sites.

C. Emission intensities as a function of laser fluence

The effective surface temperature of the neutral particles, generated by the laser pulse, is a strong function of laser fluence. Effective surface temperatures derived from measurements on both Na° and Cl° with a background substrate temperature at 28 °C (room temperature) are shown in Fig. 3(a). First, we see that for a given fluence, the two masses yield nearly the same temperature. The small but systematic difference between the two effective temperatures ($T_{\mathrm{Cl}} < T_{\mathrm{Na}}$) derived from the Na° and Cl° emissions, respectively, is consistent with a small contribution to the signal at 35 amu/e due to a measurable cracking fraction from molecular chlorine (Cl_2); this added component in the detected signal shifts the measured TOF at 35 amu/e to slightly longer times. The good agreement between effective temperatures calculated from Na° and Cl° is strong evidence for both atomic emission species being in quasithermal equilibrium with a hot surface.

When the emission intensities are plotted in Arrhenius form against the effective surface temperature derived from the time-of-flight signals taken at different laser fluences, we find that both emissions again exhibit Arrhenius-like behavior. The two slopes of the curves in Fig. 3(b) yield independently an activation energy of 0.30 eV for both species. This suggests that the atomic Na° and Cl° emissions are both rate limited by the same thermally activated process, different from that induced by background crystal temperature. This activation energy can be reduced by deliberately introducing water vapor into the vacuum system, indicating that the thermally activated step takes place at or very near the surface.

Höche *et al.* observe a very similar activation energy for layer-by-layer removal of NaCl from single-crystal sodium chloride exposed to vacuum-ultraviolet radiation from a deuterium lamp. Höche *et al.* monitored material removal by helium atom scattering as a function of time and substrate temperature. For substrate temperatures between 250 and 400 K, they found an apparent thermal activation energy for layer removal of 0.27 ± 0.02 eV. Consistent with the general trend observed by Höche *et al.*, our time-of-flight measurements of laser-induced emissions at higher substrate temperatures show higher activation energies. Total emission intensities from a substrate held at 800 K are plotted against the effective surface temperature (due to laser heating) in Fig. 4. Again, the emission intensities show Arrhenius behavior, with activation energies of 0.35 eV for atomic chlorine and 0.41 eV for atomic sodium. The higher, distinct activa-

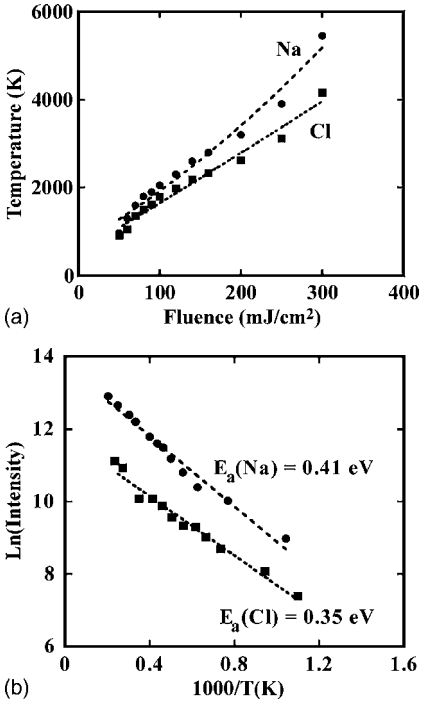

FIG. 4. (a) Effective surface temperatures derived from Maxwell–Boltzmann fits to Na° and Cl° time-of-flight data vs fluence and (b) Arrhenius plots of the emission intensities vs effective surface temperature. The background surface temperature was 800 K.

tion energies measured for the two emissions suggest that the rate-limiting, thermally assisted step has changed and is no longer the same for the two emissions.

D. Surface topography

Surface features produced by 50 pulses of 248-nm radiation at fluences of 80 and 120 mJ/cm^2 are shown in Fig. 5. Both images show high densities of monolayer islands and significant erosion along cleavage steps. The island distribution is rather uniform, except near cleavage steps, where they are depleted. The average island step height of 0.29 ± 0.02 nm is consistent with the 0.28-nm steps expected for a single-monolayer NaCl island and inconsistent with metallic Na islands. Islands of metallic Na on NaCl are expected to have heights on the order of 0.35 nm.[13] In addition, the surface treated at 120 mJ/cm^2 shows several monolayer-deep pits. These laser-induced pits are similar to monolayer etch pits produced by UV and electron irradiation at low doses on KBr (Refs. 11, 12, 14, and 15) and KI (Ref. 16) by Szymonski *et al.* Observations as a function of laser fluence show that the islands appear before the pits. Therefore, we cannot attribute islands to the material left behind from surrounding monolayer desorption.

Cleavage steps that have not been exposed to the laser are quite smooth on the micron scale. Both the steps and islands on irradiated surfaces are jagged on the micron scale, suggesting that material has been removed. This observation suggests that the islands are formed by aggregation of material detached from cleavage steps. Similar islands have not been observed after electron irradiation, by us or by others, suggesting that the high temperatures produced by the laser

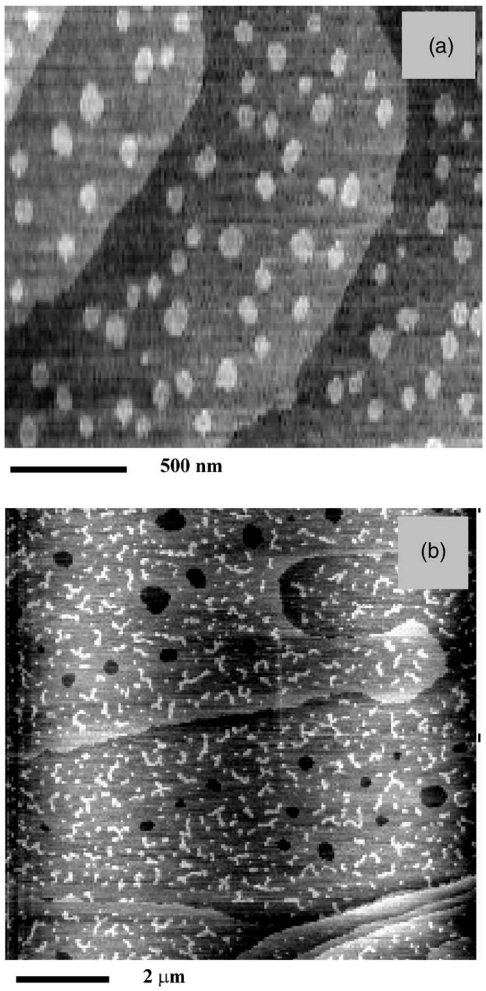

FIG. 5. Atomic force microscope images of single-crystal NaCl exposed to 50 pulses of 248-nm radiation at (a) 80 m/cm^2 and (b) 120 mJ/cm^2. Note the contrasting scales of the two images.

play an important role in cleavage step erosion and island formation—consistent with a thermally assisted, photoelectronic erosion process from step edges. The island growth consists of material that has not desorbed from the surface, but has migrated by surface diffusion, resulting in nucleation and growth of the islands. The round island structures, even in the vicinity of steps, suggests that impingement into the islands is occurring from all directions.

IV. DISCUSSION

A. Role of *F-H* pair production

Defect production during electron and photon irradiation of the alkali halides has been extensively studied. Significant reviews of theoretical and experimental results include Refs. 3, 4, and 6. Electron-hole recombination, in particular, produces self-trapped holes that can decay into isolated *F* centers (anion vacancies with a trapped electron) and *H* centers (Cl_2^- on the anion sublattice). Near room temperature this process has an apparent thermal activation energy of 0.07 eV.[17] This agrees well with the activation energy derived from the variation of emission intensity at both 23 and 35 amu/*e* with background substrate temperature at constant

laser fluence. Thus it is likely that one rate-controlling step in the emission process is *F-H*-center pair production.

Significantly, the photon energy employed in this work (5.0 eV) is insufficient to produce electron-hole pairs in the bulk or on the ideal surface by single-photon excitation.[18] Excitations across the NaCl band gap require two photons at 248 nm, and occur with relatively low probability. Multiphoton absorption across the band gap is expected to absorb 0.01–0.1% of the total incident laser flux at the low power densities employed in this work (<20 MW/cm^2). Therefore, photon absorption in this work is dominated by defects. Nevertheless, the total number of electron-hole pairs produced by two-photon absorption can be substantial. Further, most of the electron-hole pairs created by two photon absorption would be produced hundreds of microns below the surface, where the temperature is close to the ambient, background sample temperature. The recombination of electrons and holes produced by single-photon absorption can then produce the self-trapped excitons required for *F-H* pair production at the cost of two or more 5-eV photons. In previous work at higher fluences, we observed the characteristic luminescence of the self-trapped exciton in NaCl at 230 and 360 nm during irradiation at 248 nm; exciton production is again attributed to electron-hole recombination.[1]

The correlation of emission intensity with background substrate temperature strongly suggests that the relevant defect formation occurs at these low temperatures, and not at the high temperatures reached during the laser pulse. If most of the laser light absorption is concentrated near the surface at cleavage-induced defects, the temperature of the sample interior during the laser pulse would be much cooler than the measured effective surface temperature. Alternatively, *F-H* pair production occurs well after the pulse, after the sample has had time to cool, due to slow charge transport and delayed electron-hole recombination. In either case, *F-H* pair production in the bulk proceeds at temperatures close to the background sample temperature.

In order to contribute to emission processes, the *F* and/or *H* centers must either be created at or transported to the surface. The diffusion of excitons or *H* centers to the surface can yield halogen emission.[7–9] Similar emissions may contribute to the departure of our time-of-flight signals from ideal Maxwell–Boltzmann behavior. However, neither of these processes can account for Na° emission. Given the similar behavior of the Na° and Cl° emissions in this work, the great majority of both emissions must be attributed to another mechanism.

The principal role of *F-H* pair production on atomic emissions most likely involves the diffusion of *F* centers to the surface, where they nucleate double kinks along the surface steps and pits on terrace sites. The pits in the AFM image of Fig. 5 were most likely formed by *F*-center aggregation,[10,11] followed by emission of the associated sodium. Initially, these *F* centers are formed in the sample interior and diffuse to the surface.[19] Kink and pit nucleation play critical roles in the evaporation of many materials[20] and require considerable energy in rocksalt structure materials.[21] The diffusion of *F* centers to step and terrace sites greatly reduces the thermal energy required for kink and pit nucleation. Molecular dynamics simulations suggest that *F* centers in NaCl are mobile in their excited states, but immobile in their ground state.[19] If so the excitation of preexisting *F* centers in the bulk plays an important role in facilitating transport to the surface.

B. Role of defect diffusion along steps

An activation energy of 0.30 ± 0.02 eV was determined for neutral emission from room-temperature substrates using the effective temperature of the particle time of flight (Fig. 3). Significantly, Höche *et al.* reported layer-by-layer removal of material from single-crystal NaCl during continuous vacuum-ultraviolet (vuv) irradiation with an activation energy of 0.27 ± 0.02 eV for substrate temperatures below 400 K.[10] Mass spectrometer observations of emissions under the conditions of their work identified molecular NaCl as a major emission component. Höche *et al.* identified this activation energy with the desorption of neutral NaCl units from the NaCl surface. As noted above, molecular NaCl is a relatively minor emission component in our laser-induced emissions, and fails to account for our atomic Na° and Cl° signals.

Significantly, Höche *et al.* also found that their helium atom scattering signals recovered after turning off their UV source, with an effective activation energy of 0.30 eV. Although they were not able to identify this activation energy with a specific, atomic-scale process, molecular-dynamics simulations associate the recovery of the helium atom scattering signal with step straightening. When the UV source is turned off, defect diffusion along the step removes many of the curves and kinks that develop during irradiation. Significantly, quadrupole-mass-selected NaCl emission ceased almost immediately when the UV source was switched off. Thus particle emission involves both thermally activated diffusion and UV excitation. For instance, atomic and molecular emissions may result from the photoelectronic excitation of structures produced by diffusion along steps.

In contrast with the continuous emissions observed by Höche *et al.*, the transient emissions produced by pulsed laser radiation involve surfaces heated to extremely high temperatures for very short times. At sufficiently high temperatures, emission of atomic species will be favored over molecular species. This would account for the atomic Na° and Cl° emissions produced by pulsed laser irradiation, as opposed to the principally molecular emissions observed under continuous vuv irradiation. If the duration of laser-induced heating were not so short, particle emission would quickly deplete the surface of participating defects. Thus the 0.30-eV activation energy process observed by Höche *et al.* was observed only at substrate temperatures less than 400 K. Under pulsed laser radiation, a similar process operates under transient heating to temperatures as high as 3000 K.

Theoretical investigations by Puchin *et al.* support the hypothesis that electronic excitations at defect structures can lead to desorption. For instance, the low coordination of ions at kink sites significantly reduces the energy required for photoelectronic excitation.[19] Unrestricted Hartree–Fock calculations of the energy required to produce a band-gap-like

excitation at a kink site by Puchin *et al.* yield a value of 5.2 eV; calculations using the same method yield 7.4 eV for sites in the bulk.[19] Although the energy required to excite ions at kink sites is still somewhat greater than the 5-eV photon energies employed in this work, low-coordinated structures are clearly favorable sites for photoelectronic excitation. Interestingly, Puchin *et al.* found no obvious barrier to the emission of neutral Na° from the excited kink state. Although this particular excitation does not account for the atomic and molecular emissions reported above, it does support the plausibility of photoelectronic emission from defect sites along steps.

C. Emission mechanisms at high background substrate temperatures

At low temperatures, photon and electron irradiation of alkali halides can preferentially desorb the halogen, resulting in the accumulation of alkali on the surface. Cation accumulation has been observed by Auger electron spectroscopy of electron-irradiated NaCl,[22] and features attributed to alkali clusters have been observed by atomic force microscopy of both electron- and photon-irradiated alkali halides.[23,24] Steady-state electron-stimulated desorption of NaCl is observed at temperatures above 550 K, which is apparently sufficient to remove neutral sodium from the surface.[22] In the present work, laser-induced heating during the laser pulse is more than sufficient to maintain approximate surface stoichiometry, allowing for sustained emission of both alkali and halogen components.

Important changes in laser-induced emission occur between 300 and 800 K, as indicated by an increase in the apparent activation energy of the thermally assisted, photoelectronic process. We attribute the apparent change in emission mechanism to the desorption or diffusion of weakly bound species *between* laser pulses. Sublimation of single-crystal NaCl (activation energy 2.2 eV) can be detected in vacuum at temperatures as low as 600 K in the absence of radiation.[10] Under these conditions, isolated ions or molecules adsorbed on terrace or step sites will be depleted between laser pulses. To maintain emission at higher substrate temperatures, processes with higher activation energies must come into play.

D. Role of neutral emissions in laser ablation

Both ion and neutral emissions are required to produce optical breakdown in ionic, optical materials.[25,26] Significant ion densities are required to provide a potential well for the accompanying electrons. Electrons entering this potential well can be accelerated to several eV. Optical breakdown occurs when neutral atoms and molecules are ionized by electron impact, dramatically increasing the local charge densities. In the absence of neutral emissions, optical breakdown is not observed. Since both ion and neutral emissions are sensitive to the presence of surface defects, surface defects can drastically lower the laser fluence required for optical breakdown. When reproducible ablation behavior is required, as in thin-film deposition, maintaining a stable defect distribution may be critical.

V. CONCLUSION

Neutral emission from single-crystal NaCl during pulsed excimer radiation at 248 nm involves at least two independent processes, both of which are observed at lower temperatures during steady-state UV radiation. We observe a thermally activated step with an activation energy of 0.07 eV that scales with the background temperature and corresponds to *F-H* center production in the bulk. *F*-center diffusion to the surface provides low-energy paths to kink and pit nucleation—key processes in material removal. A second, thermally assisted, photoelectronic process displays an apparent activation energy of 0.30 ± 0.02 eV, where the temperature corresponds to the peak temperature during the laser pulse. Comparison with the helium scattering and emission measurements of Höche *et al.* during continuous vuv irradiation suggests that the responsible process involves a structure produced by thermal diffusion along the step which yields emission after excitation by UV photons. It is not clear whether particles desorb directly into vacuum, or onto terrace sites for later desorption into vacuum. The appearance of NaCl islands on excimer-irradiated surfaces suggests that significant numbers of particles are desorbed from steps onto terraces sites. Islands are then formed by aggregation.

The short pulses and high temperatures produced by excimer laser radiation provide significant experimental challenges to the identification of emission mechanisms. Nevertheless, these emissions play an important role in laser damage and ablation processes. Pulsed excimer lasers remain the most economical source of monoenergetic photons in much of the ultraviolet portion of the spectrum. Understanding these emission mechanisms is important to the design of damage-resistant optical materials and components, as well as the controlled emissions desired in laser ablation for thin-film deposition and chemical analysis.

ACKNOWLEDGMENTS

This work was supported by the Department of Energy under Contract No. DE-FG02-04ER15618. We also wish to thank Loren Cramer for his frequent assistance in the laboratory.

[1] R. L. Webb, L. C. Jensen, S. C. Langford, and J. T. Dickinson, J. Appl. Phys. **74**, 2338 (1993).
[2] C. Bandis, S. C. Langford, and J. T. Dickinson, Appl. Phys. Lett. **76**, 421 (2000).
[3] F. Seitz, Rev. Mod. Phys. **26**, 7 (1954).
[4] N. Itoh, Adv. Phys. **31**, 491 (1982).
[5] R. T. Williams, Radiat. Eff. Defects Solids **109**, 175 (1989).
[6] N. Itoh and M. Stoneham, *Materials Modification by Electronic Excitation* (Cambridge University, Cambridge, UK, 2000).
[7] A. Schmid, P. Bräunlich, and P. K. Rol, Phys. Rev. Lett. **35**, 1382 (1975).
[8] P. D. Townsend, R. Browning, D. J. Garlant, J. C. Kelly, A. Mahjoobi, A. J. Michael, and M. Saidoh, Radiat. Eff. **30**, 55 (1976).
[9] W. P. Hess, A. G. Joly, D. P. Gerrity, K. M. Beck, P. V. Sushko, and A. L. Shluger, J. Chem. Phys. **115**, 9463 (2001).
[10] H. Höche, J. P. Toennies, and R. Vollmer, Phys. Rev. B **50**, 679 (1994).
[11] B. Such, P. Czuba, P. Piatkowski, and M. Szymonski, Surf. Sci. **451**, 203 (2000).
[12] M. Szymonski, J. Kolodziej, B. Such, P. Piatkowski, P. Struski, P. Czuba, and F. Krok, Prog. Surf. Sci. **67**, 123 (2001).
[13] H. Häkkinen and M. Manninen, J. Chem. Phys. **105**, 10565 (1996).
[14] B. Such, J. Kolodziej, P. Czuba, P. Piatkowski, P. Struski, F. Krok, and M. Szymonski, Phys. Rev. Lett. **85**, 2621 (2000).

[15]R. Bennewitz *et al.*, Surf. Sci. **474**, L197 (2001).
[16]R. M. Wilson, W. E. Pendleton, and R. T. Williams, Radiat. Eff. Defects Solids **128**, 79 (1994).
[17]E. Sonder and W. A. Sibley, in *Point Defects in Solids*, edited by J. H. Crawford and L. M. Slifkin (Plenum, New York, 1972), pp. 201–290.
[18]V. E. Puchin, A. L. Shluger, and N. Itoh, Phys. Rev. B **47**, 10760 (1993).
[19]V. Puchin, A. Shluger, Y. Nakai, and N. Itoh, Phys. Rev. B **49**, 11364 (1994).
[20]J. P. Hirth and G. M. Pound, J. Chem. Phys. **26**, 1216 (1957).
[21]J. Magill, J. Bloem, and R. W. Ohse, J. Chem. Phys. **76**, 6227 (1982).
[22]M. Szymonski, J. Ruthowski, A. Poradzisz, Z. Postawa, and B. Jørgensen, in *Desorption Induced by Electronic Transitions-DIET II* (Springer, Berlin, 1985), pp. 160–168.
[23]R. M. Wilson and R. T. Williams, Nucl. Instrum. Methods Phys. Res. B **101**, 122 (1995).
[24]K. Miura and K. Maeda, Nucl. Instrum. Methods Phys. Res. B **116**, 486 (1996).
[25]J. J. Shin, D. R. Ermer, S. C. Langford, and J. T. Dickinson, Appl. Phys. A **64**, 7 (1997).
[26]D. R. Ermer, S. C. Langford, and J. T. Dickinson, J. Appl. Phys. **81**, 1495 (1997).